

# Influence of Magnesium Cations on the Electrochemical Behavior of the Ti(IV)/Ti(III) Redox Couple in Alkali Chloride-Fluoride Melt: Experimental and Quantum-Chemical Studies

V. G. Kremenetsky, D. A. Vetrova, and S. A. Kuznetsov\*

Tananaev Institute of Chemistry and Technology of the Federal Research Centre “Kola Science Centre of the Russian Academy of Sciences”, 26a Akademgorodok, 184209 Apatity, Murmansk region, Russia

\*E-mail: [kuznet@chemy.kolasc.net.ru](mailto:kuznet@chemy.kolasc.net.ru)

Received: 14 April 2018 / Accepted: 17 May 2018 / Published: 5 July 2018

---

The influence of  $\text{Mg}^{2+}$  cations on the charge transfer kinetics of the redox couple Ti(IV)/Ti(III) was studied by cyclic voltammetry. The standard rate constants of charge transfer ( $k_s$ ) for the redox couple Ti(IV)/Ti(III) in the NaCl-KCl (equimolar mixture)-NaF(10 wt.%) $-\text{K}_2\text{TiF}_6$  melt upon the addition of  $\text{Mg}^{2+}$  cations into the initial melt were calculated based on the Nicholson's equation. The temperature dependence of  $k_s$  for molten salt system with additions of  $\text{Mg}^{2+}$  cations was determined and the activation energy of charge transfer was calculated. Based on the experimental data and the quantum-chemical analysis of the frontier molecular orbitals in the  $\text{MgTiF}_6 + 12\text{MgCl}_2$  system, a mechanism for electrochemical charge transfer was proposed. The geometric structure of the transition state was shown to be not intermediate between the initial and final states of the system. This approach can be recommended as a tool for verifying hypotheses related to the mechanism of electrochemical electron transfer.

---

**Keywords:** Molten Salt, Redox Couple, Standard Rate Constants of Charge Transfer, Quantum-Chemical Analysis, Frontier Orbitals.

## 1. INTRODUCTION

Electrochemical behavior of titanium in molten salts has been goal of many studies. This is due to wide titanium alloys using in modern technology in particular in aerospace and aircraft industry, atomic power engineering and electronics. To perform an electrochemical synthesis of titanium alloys in molten salts, it is necessary to know the electrochemical behavior of titanium. The electrode processes and the diffusion coefficients of titanium complexes in various oxidation states were studied

[1-3]. However, the systematic investigation of the second coordination sphere composition influence on the standard rate constants of charge transfer ( $k_s$ ) for the redox couple Ti(IV)/Ti(III) is lacking.

The second coordination sphere composition influence on the standard rate constants of charge transfer in alkali chloride melts was studied for the redox couple Eu(III)/Eu(II) [4, 5], Sm(III)/Sm(II) and Yb(III)/Yb(II) [6]. It was shown that the  $k_s$  values rise with increasing of the outer-sphere cation size from sodium to cesium in all cases. It was assumed that charge transfer in the above couples occurs through the outer-sphere cation. The highest  $k_s$  values obtained for CsCl were explained by its higher polarizability than other alkali cations.

The method of cyclic voltammetry was used to determine the standard rate constants of charge transfer of the redox couples Nb(V)/Nb(IV) [7-13] and Cr(III)/Cr(II) [14-16] in alkali chloride melts. The quantum-chemical calculations showed [11] that the values of the charge transfer activation energy might indeed change nonmonotonously in the series of Na-K-Cs in accordance with the ratio of reorganization energies that leads to nonmonotonic variation of the standard rate constants.

However, influence of the second coordination sphere on the standard rate constants of charge transfer cannot be prognosticated a priori.

An experimental study of the charge transfer mechanism in molten salts is a difficult task. In this case, it is expedient to use additionally quantum-chemical methods for analysis of suitable model systems. However, there are own problems. As our experience shows, model systems assigned to investigate the mechanism of charge transfer must include, in addition to the electroactive complex, two more of its coordination spheres. For electrolytes based on alkaline earth metal halides, this can be, for example,  $MTiF_6 + 12MX_2$  type systems (M – Mg, Ca, Sr, Ba; X – F, Cl). A direct search for a transition state in such system requires the addition of a cluster that simulates the electrode surface. In the case of a carbon cluster, at least 200 carbon atoms are necessary. The search for a transition state by standard methods will require enormous computer time and is almost unrealistic. For this reason, there are no such quantum-chemical studies in the world literature.

In this paper, we proposed a different approach, which is based on the analysis of frontier molecular orbitals under various deformations of the initial structure. Molecular orbital (MO), which are close in energy to the frontier molecular orbitals, are also included in the consideration. In this work, we proposed also to use the method of frontier molecular orbitals for analysis possible variants of electron transfer in electrochemical systems. The using of this method makes it possible to obtain extremely useful information about the possibility or impossibility of one or another mechanism of electron transfer. This method allow to turn the discussion about possible mechanisms of charge transfer in electrochemical systems to a deeper level, for example, from a simple statement of the fact of charge transfer by a bridging mechanism to the analysis of specific variants of such transfer.

After the pioneer work of Fukui et al. [17] analysis of frontier orbitals began to be widely used in various fields of chemistry, including electrochemistry [18-21]. However, the type of the frontier orbitals is not considered as a key characteristic when solving the problem of the possibility of electron transfer to an electroactive particle.

The goal of the present investigation was to study the influence of  $Mg^{2+}$  cations having a high ionic potential on the standard rate constants of charge transfer for the Ti(IV)/Ti(III) redox couple in the NaCl-KCl (equimolar mixture)-NaF(10 wt.%) -  $K_2TiF_6$  melt.

The aim of the quantum-chemical part of this work – to show the need of verification of any charge transfer mechanism, and to demonstrate that, based on the analysis of the frontier orbital nature, it is possible to indicate the most probable mechanism of electron transfer (ET) in electrochemical reactions without excessive expenditure of computer time. As an example, the model system  $\text{MgTiF}_6 + 12\text{MgCl}_2$  was used. The choice of the research strategy was based on the results of an experimental determination of the standard rate constants and activation energy of charge transfer.

## 2. EXPERIMENTAL

### 2.1 Chemicals

The preparation of alkali chlorides (NaCl, KCl) and sodium fluoride was described in [22].

Potassium hexafluorotitanate of pure grade was dissolved in hot water (363-373 K) and the solution was passed through a hot filter and cooled. The resulting  $\text{K}_2\text{TiF}_6$  crystals were dried in a vacuum, first at 363 K for 24 h and then at 423 K for 6 h [23].

Anhydrous magnesium chloride ( $\geq 98\%$ , Sigma) was used without additional treatment.

### 2.2 Apparatus and equipment

Cyclic voltammetry was employed, using a VoltaLab-40 potentiostat with complementarily packaged software “VoltaMaster 4”, version 6. The potential scan rate ( $v$ ) was varied between 0.1 to 2.0  $\text{V s}^{-1}$ . Experiments were carried out in the temperature range 723-1173 K. The voltammetric curves were recorded at a glassy carbon electrode (1.0 and 2.0 mm diameter) with respect to a glassy carbon plate quasi-reference electrode. The glassy carbon ampoule served as the counter electrode. While the potential of this quasi-reference electrode does not constitute a thermodynamic reference, the use of this electrode was preferred in order to avoid any contact between the melt and oxygen-containing material as used in the classical reference electrodes. A Ag/NaCl-KCl-AgCl (2 wt%) reference electrode was used in order to obtain more reliable potential values. At the final stage of each experimental set, this reference electrode was immersed in the melt for a short time and the standard rate constant was determined, the melt being no longer used after these measurements [5, 24]. A good agreement was observed between the values of  $k_s$  obtained with a silver chloride reference electrode and a glassy carbon quasi-reference electrode.

### 2.3 The procedure for the determining of the standard rate constants of charge transfer

Nicholson [25] derived theory for the determining of the standard rate constants of charge transfer for quasi-reversible redox process, not complicated by insoluble product formation, from cyclic voltammetry data. When the Ox and Red forms either are soluble in solution or in the electrode material and are transferred by diffusion only, the solution of the problem cannot be expressed in

analytical form. In study [25] was found the correlation between the  $\Psi_T$  function connected with the cathodic and anodic peak potential separation  $\Delta E_p$  and the standard rate constant of charge transfer:

$$\Psi_T = \frac{k_s (D_{ox} / D_{red})^{\alpha/2}}{\sqrt{(\pi D_{ox} n F v) / RT}}, \quad (1)$$

where  $\alpha$  is the transfer coefficient,  $n$  is the number of electrons involved in the reaction.

The value of  $\alpha = 0.5$  is used in Equation 1 because the original work [25] gives the correlation between the  $\Psi$  and  $\Delta E_p$  functions for this value.

To calculate the standard rate constant of charge transfer, the values of  $(\Delta E_p)_T$  and  $\Psi_T$  are required. In [25] they are given for 298 K and thus must be recalculated for the operation temperature. The recalculation was conducted by the following equations [26]:

$$(\Delta E_p)_{298} = (\Delta E_p)_T 298/T, \quad (2)$$

$$\Psi_T = \Psi_{298} \sqrt{T/298}. \quad (3)$$

From the values of  $\Psi_T$  function, obtained according to Equations 2 and 3, we calculated the standard rate constants of charge transfer for the Ti(IV)/Ti(III) redox couple by using (1) and the diffusion coefficients.

## 2.4 Computational methods

The geometry optimization of structures was performed with the Firefly quantum-chemical program package [27], partially based on the codes of the GAMESS(US) program [28], by the density functional theory DFT method with the use of the hybrid functional B3LYP. Quasi-relativistic ECP basis of the Stuttgart/Cologne group was used for Ti (Stuttgart RSC 1997 ECP) and F, Cl (Stuttgart RLC ECP). For Mg, the ECP basis set Crenbl was used [29-31]. An electric field with a strength  $10^9 \text{ V m}^{-1}$  imitating the cathode field was applied to all model systems [32].

## 3. RESULTS AND DISCUSSION

### 3.1 Electrochemical studies

The typical voltammetric curves for the Ti(IV)/Ti(III) redox couple obtained at the glassy carbon electrode upon the introduction of magnesium chloride into the initial melt are presented in Fig. 1.

Because the procedure used to calculate the standard charge-transfer rate constants is valid only for quasi-reversible processes, it is necessary to determine the range of polarization rates where the process:



is quasi-reversible.

The dependences of the cathodic peak current and potential on the polarization rate (Fig. 2) were studied to determine the quasi-reversibility region of the process in the  $(\text{NaCl-KCl})_{\text{eqimol}}\text{-NaF}$  (10

wt %)-K<sub>2</sub>TiF<sub>6</sub>-MgCl<sub>2</sub> melt. According to voltammetry diagnostic criteria the deviation of the experimental points from a straight line in Fig. 2a at a polarization rate higher than 1.0 V s<sup>-1</sup> indicates that the electroreduction of titanium at higher polarization rates is quasi-reversible. This is also confirmed by the curvilinear dependence of  $E_p(C)$  on  $\log v$  (Fig. 2b).

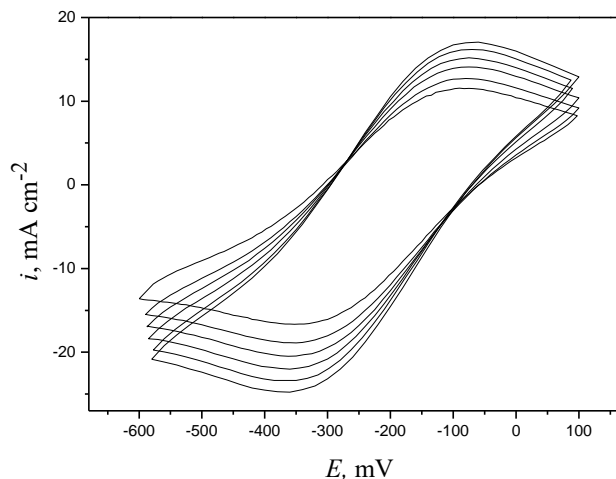


**Figure 1.** Cyclic voltammograms of (NaCl–KCl)<sub>eqimol</sub>-NaF (10 wt %)-K<sub>2</sub>TiF<sub>6</sub>-MgCl<sub>2</sub> melt. The polarization rates are (internal curve) 0.75 and (external curve) 1.0, 1.25, 1.5, 1.75, and 2.0 V s<sup>-1</sup>. Temperature 1023 K.

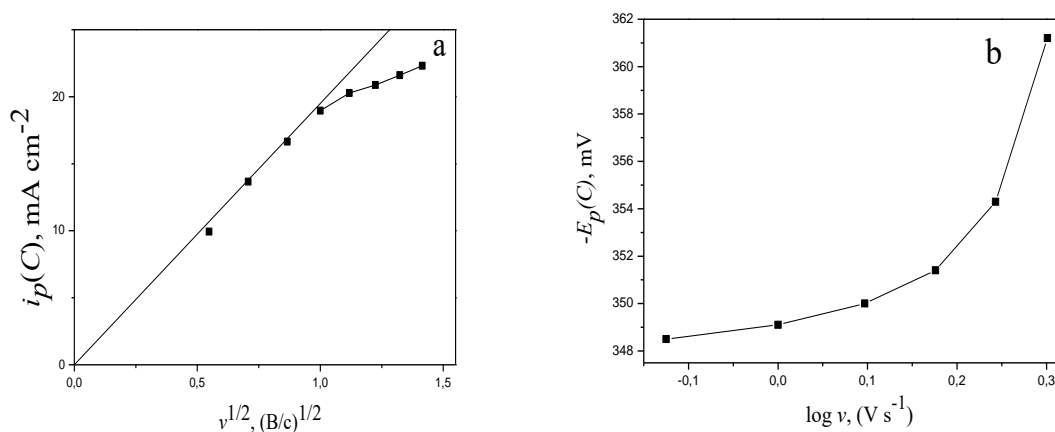


**Figure 2.** Peak current (a) and peak potential (b) of the Ti(IV) to Ti(III) electroreduction vs. the polarization rate in the (NaCl–KCl)<sub>eqimol</sub>-NaF(10 wt %)-K<sub>2</sub>TiF<sub>6</sub>-MgCl<sub>2</sub> melt. Temperature 1023 K.

The values of function  $\psi_T$  obtained according to (2) and (3) made it possible to calculate the standard rate constants of charge transfer for the Ti(IV)/Ti(III) redox couple using the values of Ti(IV), Ti(III) diffusion coefficients [33].

The study of the influence of the Mg<sup>2+</sup> strongly polarizing cations on the standard constants for the Ti(IV)/Ti(III) redox couple showed that  $k_s$  increased upon the introduction of MgCl<sub>2</sub> additives into the starting melt and reached a maximum at a certain Mg<sup>2+</sup>/Ti(IV) ratio (Fig. 3).

An increase in  $k_s$  is related to the displacement of sodium and potassium cations by  $Mg^{2+}$  cations from the second coordination sphere of the titanium complexes, resulting in the enhancement of the counter-polarization effect due to their higher ionic potential, elongation of the bond lengths between titanium and the fluoride ligands, and weakening of the titanium fluoride complexes. The further additives of the salt resulted in some decrease in  $k_s$ . Decrease of  $k_s$  at the definite ratio of components can be explained by increase of the melts viscosity (viscosity of  $MgCl_2$  is higher than alkali metal chlorides [34]), which brings to decreasing of the diffusion coefficients.

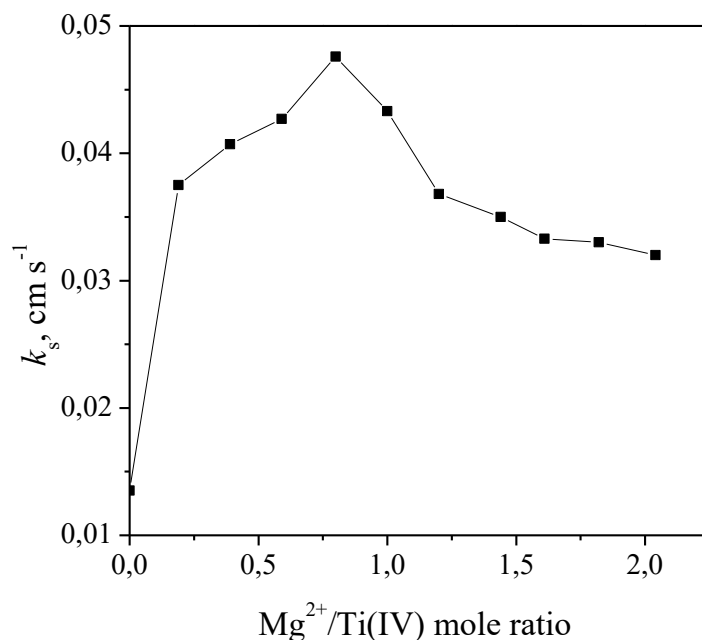


**Figure 3.** The dependence of  $k_s$  on the  $Mg^{2+}/Ti(IV)$  mole ratio in the  $(NaCl-KCl)_{eqimol}-NaF$  (10 wt %)- $K_2TiF_6$  melt. Temperature 1023 K. Scan rate  $1.5 V s^{-1}$ .

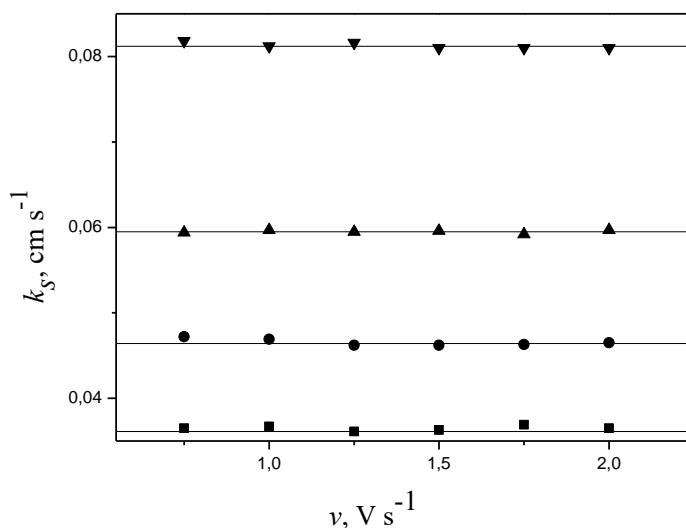


**Figure 4.** Standard rate constants of charge transfer rate ( $k_s$ ) on the sweep rate ( $v$ ) for different temperatures in the  $(NaCl-KCl)_{eqimol}-NaF$  (10 wt %)- $K_2TiF_6-MgCl_2$  melt.

The temperature dependences of the maximum values of  $k_s$  at different polarization rates for the system with magnesium chloride additives are presented in Fig. 4. As can be seen from Fig. 4, the standard rate constants of charge transfer rate for the Ti(IV)/Ti(III) redox couple are independent of the polarization rate and increase with temperature. An increase in  $k_s$  with temperature is due to an increase in the thermal energy of the system and an increase in the fraction of particles with the energy that is necessary for overcoming an activation barrier [35].

The temperature dependence of the maximum standard rate constants of charge transfer after the addition of  $\text{Mg}^{2+}$  cations is described by the following equation:

$$\log k_{s(\text{Mg}^{2+})} = -(0.25 \pm 0.04) - (1100 \pm 230)/T \quad (5)$$

The activation energy of charge transfer was found equal to  $21 \pm 4 \text{ kJ mol}^{-1}$ , which is substantially lower than the activation energy of the initial system [23].

Let us elucidate what information can be extracted from analysis of the molecular orbital structure of the molten salt systems. As an example, consider the  $\text{MgTiF}_6 + 12\text{MgCl}_2$  model system.

### 3.2. Results of quantum-chemical analysis of the model system $\text{MgTiF}_6 + 12\text{MgCl}_2$

In this work, we were interested in the state of the complex  $\text{TiF}_6^{2-}$  near the cathode surface. For this reason, on one side of the model system, a flat boundary layer consisting of 17 chlorine and magnesium ions was formed. The titanium complex is in contact with one of the magnesium cations belonging to the boundary layer, since the dependence of the  $k_s$  value on the cation  $\text{M}^{2+}$  radius [33] indicates the bridge nature of ET to the  $\text{TiF}_6^{2-}$  complex. Such character of the  $k_s$  dependence means that during the transformation of the structure from the initial to the transition state, there is no noticeable change in the composition of the second coordination sphere of the complex.

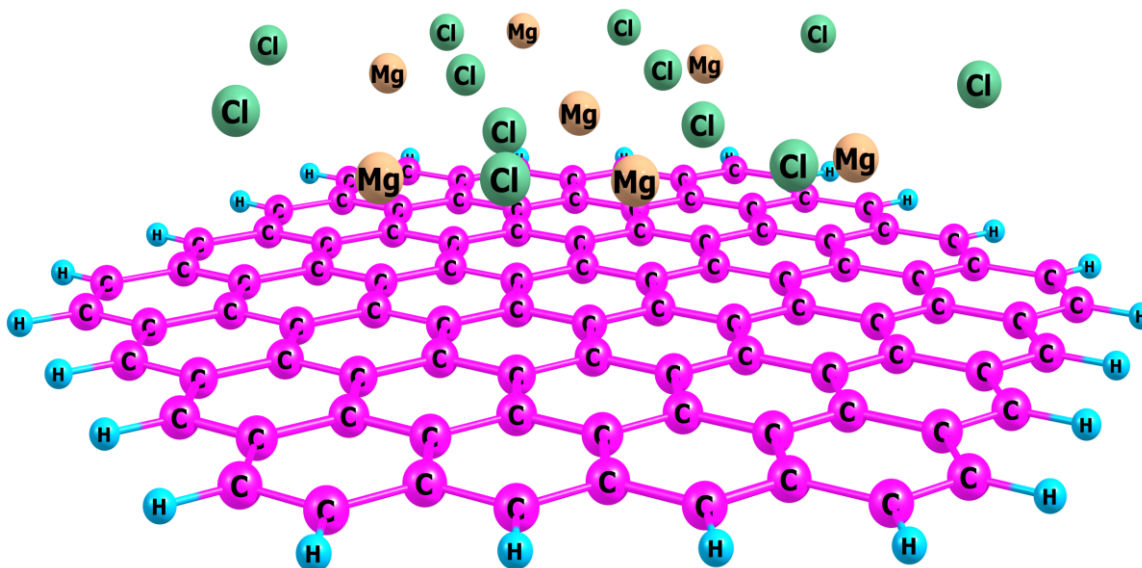


Figure 5. The structure  $\text{C}_{96}\text{H}_{24} + 7\text{MgCl}_2$ .

In general, the boundary ions of chlorine and magnesium are not in the same plane. The mutual displacement of these ions was determined from the computation in the model system  $C_{96}H_{24}+7MgCl_2$ , where  $C_{96}H_{24}$  is a flat carbon cluster simulating the surface of the cathode; hydrogen atoms close the broken bonds of carbon atoms to prevent artifacts. After optimization of this system, the chlorine anions shifted by 0.3 Å relative to the magnesium cations in the direction opposite to the surface of the carbon cluster (Fig. 5). The direction of this displacement corresponds to the effect of the electric field on the chlorine anions.

Thus, the equilibrium shift  $\Delta d$  is 0.3 Å. The model system  $MgTiF_6+12MgCl_2$  with such shift value will be considered referent.

Note that adding of  $C_{96}H_{24}$  cluster to our main system  $MgTiF_6+12MgCl_2$  would require a drastic increase in the computation time. However, for qualitative conclusions, it is sufficient to analyze  $MgTiF_6+12MgCl_2$  system.

In further calculations, the parameter  $\Delta d$  was varied and for each  $\Delta d$  value, the system was optimized. The positive  $\Delta d$  values correspond to the shift of the boundary chlorine anions relative to the magnesium cations toward the remaining part of the system, and the negative  $\Delta d$  values indicate the opposite direction of displacement of the boundary chlorine anions (i. e. towards the cathode).

Calculations showed that when the  $\Delta d$  value changes, the energy of the system also changes. For a number of systems, the energy difference  $\Delta E$  of this and the reference system is given in Table 1.

As can be seen from the Table 1, when the chlorine anions are shifted in direction from the system, then the energy value increases in absolute value. This means that the appearance of the  $TiF_6^{2-}$  complex in the boundary layer disturbs the boundary structure, and states with negative  $\Delta d$  values become more advantageous. However, the character of the lowest unoccupied molecular orbital (LUMO) indicates that for any values of this parameter, the electron transfer to a complex by a bridge mechanism is impossible in such systems. An example of LUMO for one of such systems is shown in Fig. 6.

The solid lines show the boundaries of the plane layer of the system. The F-Mg bridge is shown in a dotted line.

As can be seen from this Figure, the wave function is localized on the complex  $TiF_6^{2-}$ , while for the electron transfer along the bridge mechanism it must be delocalized between the complex and the bridge cation of magnesium.

Intermediate structures, in which the Ti-F bond lengths are larger than in the initial (before ET) and less than in the final (after ET) structures, give the LUMO type shown in Fig. 6, that is, in these states, the bridge ET is also impossible. The same type of LUMO has structures of a mixed type, in which some of the Ti-F bonds are larger than in the initial structure, and some less.

A systematic study of the influence of the  $\Delta d$  value and the length of Ti-F bonds on the LUMO character showed the following: 1) the group of lower free MOs, the main contribution to which gives the  $TiF_6^{2-}$  complex, is destabilized with increasing of Ti-F bond contraction ( $\Delta r$ ); 2) when the shift  $\Delta d$  increases, this MO group is also destabilized and simultaneously free MOs belonging to the boundary ions become more stable. In particular, when the Ti-F bonds are compressed on  $\Delta r = 0.05$  Å, the critical value of the shift  $\Delta d$  is 0.6 Å. That is, at  $\Delta d \geq 0.6$  Å and  $\Delta r = 0.05$  Å, LUMO is delocalized between the complex and the bridge cation. At excessively large values of  $\Delta d$  and  $\Delta r$ , LUMO is

completely localized on the boundary ions, but this is undesirable (see below). The combination of the parameters  $\Delta d = 0.6, 0.7 \text{ \AA}$  and  $\Delta r = 0.05 \text{ \AA}$  is optimal. At these values, LUMO is delocalized between the complex and the bridge cation and the activation energy ( $\sim 18 \text{ kJ mol}^{-1}$ ) is close to the experimental value ( $21 \pm 4 \text{ kJ mol}^{-1}$ ). An increase in the parameter  $\Delta r$  leads to a rapid increase in the activation energy, a contraction value of  $0.05 \text{ \AA}$  is optimal.

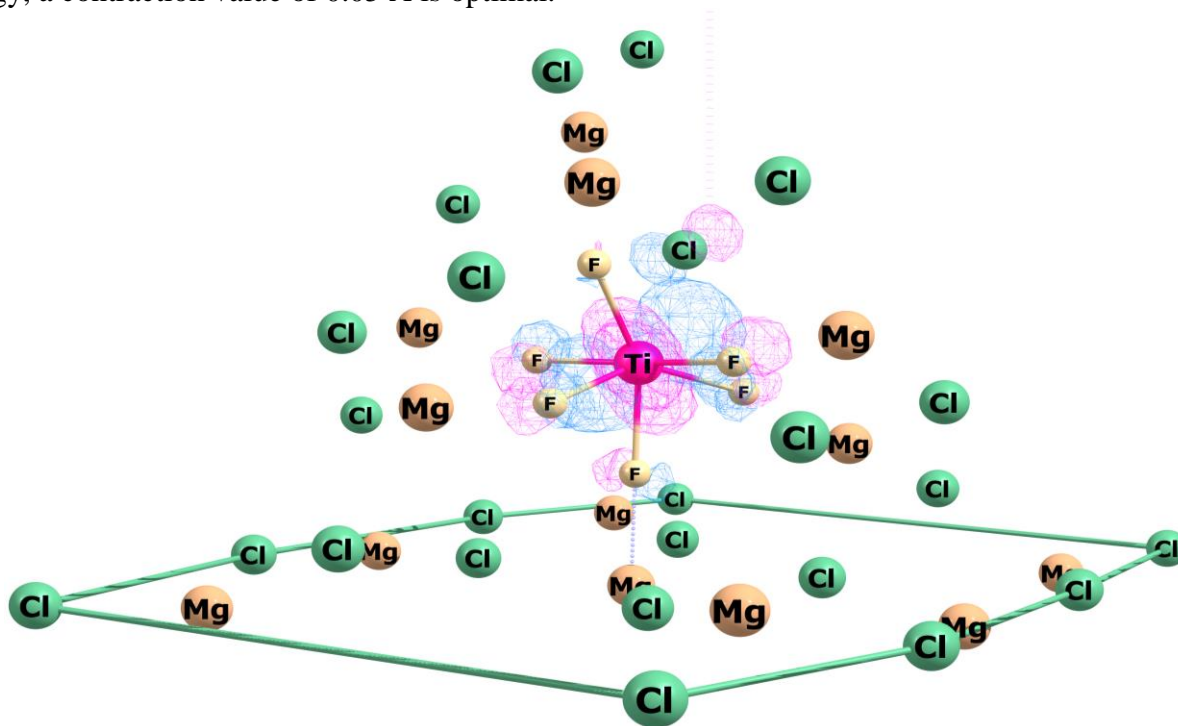


**Figure 6.** The LUMO of the structure  $\text{MgTiF}_6 + 12\text{MgCl}_2$  with  $\Delta d = 0.3 \text{ \AA}$ .

However, from the data in Table 1 it follows that the energy of states with  $\Delta d = 0.6, 0.7 \text{ \AA}$  is too large. In reality, it cannot be greater than the experimental activation energy  $E_a$ . Calculations showed that the solution to this problem are states with a mixed shift, when the boundary chlorine anions nearest to the bridge cation have a shift  $\Delta d \sim 0.75 \div 0.85 \text{ \AA}$ , and the more distant boundary anions are shifted in the opposite direction from the bridge cation with  $\Delta d \sim -0.35 \div -0.5 \text{ \AA}$ . An analysis of the electronic structure of this type systems showed that the first group of ions, consisting of 3-5 boundary chlorine anions, destabilizes the free orbitals of the  $\text{TiF}_6^{2-}$  complex relatively the free MOs of the bridge cation.

The energy of such structures is close to the energy of the reference state ( $\Delta E \sim -3 \div 5 \text{ kJ mol}^{-1}$ ), and the activation energy value is in the range of  $17\text{-}23 \text{ kJ mol}^{-1}$ , that is, close to the experimental value  $21 \pm 4 \text{ kJ mol}^{-1}$ .

An example of such structure is shown in Fig. 7. Here, the four boundary  $\text{Cl}^-$  anions closest to bridge magnesium have a shift  $0.8 \text{ \AA}$ , and the shift of the remaining  $\text{Cl}^-$  ions is  $-0.4 \text{ \AA}$ .

Structures of this type have the same type of LUMO (Fig. 7a), which is delocalized between the complex and the bridge cation of magnesium. As noted earlier, this indicates a high probability of ET from the cathode. The next unoccupied orbital (LUMO+1) is located  $8 \text{ kJ mol}^{-1}$  higher and has the same character as LUMO. At  $14\text{-}16 \text{ kJ mol}^{-1}$  higher than LUMO, there is an orbital (LUMO+2), which

belongs to the complex  $\text{TiF}_6^{2-}$ . These three orbitals can be mixed. The next orbital LUMO+3 is separated from the LUMO by a gap of 82-83  $\text{kJ mol}^{-1}$  and cannot be mixed with LUMO.

An equally important characteristic is the highest occupied molecular orbital (HOMO) type of the structure after ET (Fig. 7b). The whole group of structures with mixed shift has the same type of HOMO, which is shown in Fig. 7b. The type of this HOMO coincides with the LUMO type before ET. The spin density of an unpaired electron is distributed between titanium and the bridge cation in the ratio  $\sim 2:1$ , which also indicates a high probability of ET to the complex  $\text{TiF}_6^{2-}$ .

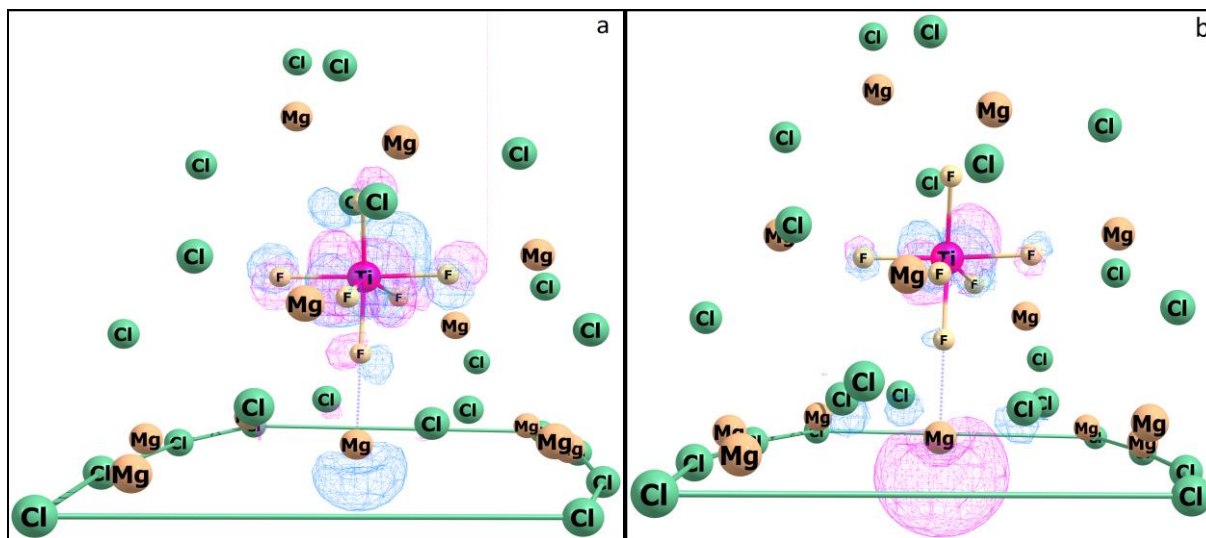


**Figure 7.** The frontier orbitals of the structure with  $\Delta d = 0.8+(-0.4)$  Å and  $\Delta r = 0.05$  Å: LUMO before electron transfer (a) and HOMO after electron transfer (b).

Theoretically, there may exist three main types of HOMO for our structures (after ET): 1) HOMO is completely localized on the boundary ions; 2) HOMO is delocalized between the boundary ions and the complex; 3) HOMO is completely localized on the complex. In the first case, probability of electron capture by the complex is very low. After diffusion of the complex into the depth of the melt, electron remains on the boundary ions and then returns to the cathode. In the second case, there is a significant probability of ET to the complex through the bridge cation. In the latter case, the probability of electron capture by the complex is close to 100%, if the complex is in contact with the surface of the electrode.

The first type of HOMO is observed when the Ti-F bonds are too strongly contracted, in this case the computed activation energy is much higher than the experimental value, although the LUMO before ET can be delocalized (but with a dominant contribution to the wave function from the boundary cations). The second type always corresponds to the same type of LUMO before ET, in this case the electron transfer to the complex by the bridge mechanism is quite real. The third case is realized when the LUMO before ET is predominantly localized on the complex. In this case, ET is impossible, since the direct access of the complex to the electrode surface is blocked by outer-sphere cations.

Thus, in a certain range of  $\Delta d$  and  $\Delta r$  values, there are such structures in the system that provide a high probability of ET from the cathode to the system. During our analysis, we considered systems with an ordered boundary layer, formed for methodological purposes. This allowed us to identify the parameters characterizing the transition state. Finally, it was found that the structure of this state is much less ordered than our initial structures of the boundary layer. This corresponds to the actual state of the boundary layer near the electrode surface. As our calculations show, the electric field of the cathode has little effect on the degree of the boundary layer ordering. The reason is a large interaction energy of ions. The action of the electric field only leads to a small perturbation of the equilibrium structure of the boundary layer and the complex. This is also indicated by the data in Table 1. It follows from them that the appearance of a complex  $\text{TiF}_6^{2-}$  in the boundary layer leads to a displacement of the boundary chlorine anions against the direction of the electric field action.

**Table 1.** The  $\Delta E$  value ( $\text{kJ mol}^{-1}$ ) at different values of the shift  $\Delta d$  ( $\text{\AA}$ ) relative to the reference state with  $\Delta d = 0.3 \text{ \AA}$

$\Delta d$	-0.3	-0.1	0.1	0.3	0.4	0.5	0.6	0.7
$\Delta E$	-152	-130	-77	0	47	102	163	232

Based on the data obtained, the charge transfer process is as follows. After diffusion into the boundary layer, the complex is waiting for a suitable environment configuration that corresponds to the transition state described above. When the transition state is reached, electron is transferred to the bridge cation and then to the complex. The required value of the Ti-F bonds contraction is achieved during a fully symmetric vibration. The probability of ET in the transition state is significant, but not equal to 100%. It depends not only on the overlapping of the bridge cation orbitals with the orbitals of the atoms on the electrode surface, but also on the probability of the transition state formation, the frequency of the fully symmetric vibration, and the probability of ET from the bridge cation to the titanium complex.

#### 4. CONCLUSIONS

The influence of the  $\text{Mg}^{2+}$  strongly polarizing cations in the NaCl-KCl (equimolar mixture)-NaF(10 wt.%) $-\text{K}_2\text{TiF}_6$  melt on the charge transfer kinetics for the Ti(IV)/Ti(III) redox couple was studied. The standard rate constants of charge transfer were shown to be independent on the polarization rate and to increase with the temperature. The increase in  $k_s$  with temperature is due to an increase in the thermal energy of the system and an increase in the fraction of particles with the energy that is necessary for overcoming the activation barrier.

An approach that indicates the way for a more detailed analysis of the mechanism of electrochemical electron transfer in molten salts was proposed. It was found that in a certain range of

structure parameters, there is a set of the system states that provides the possibility of electron transfer with an activation energy close to the experimental one.

Estimates of the activation energy and the structure of the transition state obtained by this approach are not precise. However, based on these data, standard methods of searching for a transition state can be used; however, this will require the introduction into the system a fragment imitating the surface of the electrode.

More accurate data on an electronic structure can also be obtained using higher-level methods; however, in this case, the computed time also increases sharply. In contrast to photochemical reactions, there is no need for electrochemical charge transfer, when the electron transfer mechanism is considered at a qualitative level.

#### ACKNOWLEDGMENTS

This work was supported by the Russian Foundation for Basic Research, project 15-03-02290-a.

#### References

1. L. P. Polyakova, P. T. Stangrit, and E. G. Polyakov, *Electrochim. Acta*, 31 (1986) 159.
2. C. A. Sequeira, *J. Electroanal. Chem.*, 239(1-2) (1988) 203.
3. L. P. Polyakova, P. Taxil, and E. G. Polyakov, *Alloys and Compd.*, 359 (2003) 244.
4. S. A. Kuznetsov and M. Gaune-Escard, *Z. Naturforsch.*, 57 (2002) 85.
5. S. A. Kuznetsov and M. Gaune-Escard, *J. Electroanal. Chem.*, 595 (2006) 11.
6. S. A. Kuznetsov and M. Gaune-Escard, *J. Nucl. Mater.*, 389 (2009) 108.
7. A. V. Popova and S. A. Kuznetsov, *Russ. J. Electrochem.*, 44 (2008) 992.
8. S. A. Kuznetsov, V. G. Kremenetsky, A. V. Popova, L. A. Chernenko, O. V. Kremenetskaya, and A. D. Fofanov, *Doklady Akademii Nauk*, 428(6) (2009) 770.
9. A. V. Popova, V. G. Kremenetsky, V. V. Soloviev, L. A. Chernenko, O. V. Kremenetskaya, A. D. Fofanov and S. A. Kuznetsov, *Russ. J. Electrochem.*, 46 (2010) 671.
10. A. V. Popova and S. A. Kuznetsov, *Russ. J. Electrochem.*, 48(1) (2012) 102.
11. A. V. Popova, V. G. Kremenetsky, and S. A. Kuznetsov, *Russ. J. Electrochem.*, 50(9) (2014) 807.
12. A. V. Popova and S. A. Kuznetsov, *J. Electrochem. Soc.*, 163 (2016) H53.
13. A. V. Popova, V. G. Kremenetsky, and S. A. Kuznetsov, *J. Electrochem. Soc.*, 164 (2017) H5001.
14. Yu. V. Stulov and S. A. Kuznetsov, *Rasplavy*, 6 (2010) 26.
15. Yu. V. Stulov, V. G. Kremenetsky, and S. A. Kuznetsov, *Int. J. Electrochem. Sci.*, 8 (2013) 7327.
16. Yu. V. Stulov, V. G. Kremenetsky, and S. A. Kuznetsov, *Russ. J. Electrochem.*, 50(9) (2014) 815.
17. K. Fukui, T. Yonezawa, and H. Shingu, *J. Chem. Phys.*, 20 (1952) 722.
18. F. Bouyer and G. S. Picard, *AIP Conf. Proc.*, 364 (1996) 532.
19. R. R. Nazmutdinov, G. A. Tsirlina, O. A. Petrii, Yu. I. Kharkats, and A. M. Kuznetsov *Electrochim. Acta.*, 45 (2000) 3521.
20. An. M. Kuznetsov, A. N. Maslii, and M. S. Shapnik, *Rus. J. Electrochem.*, 38, 123 (2002).
21. R. R. Nazmutdinov, G. A. Tsirlina, I. R. Manyurov, M. D. Bronshtein, N.V. Titova, and Z. V. Kuzminova, *Chemical Physics*, 326 (2006) 123.
22. G. A. Bukatova and S. A. Kuznetsov, *Electrochem. Commun.*, 7 (2005) 637.
23. D. A. Vetrova and S. A. Kuznetsov, *ECS Transactions*, 15 (2016) 363.
24. S. A. Kuznetsov and M. Gaune-Escard, *Electrochim. Acta*, 46 (2001) 1101.
25. R. S. Nicholson, *Anal. Chem.*, 37(11) (1965) 1351.
26. S. A. Kuznetsov, S. V. Kuznetsova, and P.T. Stangrit, *Russ. J. Electrochem.*, 26 (1990) 63.

27. A. A. Granovsky, <http://classic.chem.msu.su/gran/gamess/index.html> (accessed May 20, 2016).
28. M. W. Schmidt, K. K. Baldrige, J. A. Boatz, S. T. Elbert, M. S. Gordon, J. H. Jensen, S. Koseki, N. Matsunaga, K. A. Nguyen, S. Su, T. L. Windus, M. Dupuis, and J. A. Montgomery, *J. Comput. Chem.*, 14 (1993) 1347.
29. D. J. Feller, *J. Comp. Chem.*, 17 (1996) 1571.
30. K. L. Schuchardt, B. T. Didier, T. Elsethagen, L. Sun, V. Gurumoorthi, J. Chase, J. Li, and T. L. Windus, *J. Chem. Inf. Model.*, 47 (2007) 1045.
31. EMSL Basis Set Library // URL: <https://bse.pnl.gov/bse/portal>
32. Z. Galus, *Fundamentals of Electrochemical Analysis*, Ellis Horwood, (1994) London, Great Britain.
33. D. A. Vetrova and S. A. Kuznetsov, *Rasplavy*, 6 (2016) 524.
34. G. J. Jantz, *Molten Salts Handbook*, Academic Press, (1967) New York, USA.
35. B. B. Damaskin and O. A. Petrii, *Introduction into Electrochemical Kinetics*, Vysshaya Shkola, (1975) Moscow, Russia.

© 2018 The Authors. Published by ESG ([www.electrochemsci.org](http://www.electrochemsci.org)). This article is an open access article distributed under the terms and conditions of the Creative Commons Attribution license (<http://creativecommons.org/licenses/by/4.0/>).